Article

A New Tyrosinase Inhibitor from the Red Alga *Symphyocladia latiuscula* (Harvey) Yamada (Rhodomelaceae)

Pradeep Paudel [1] , Aditi Wagle [1] , Su Hui Seong [1] , Hye Jin Park [2] , Hyun Ah Jung [3],* and Jae Sue Choi [1],*

[1] Department of Food and Life Science, Pukyong National University, Busan 48513, Korea;
    phr.paudel@gmail.com (P.P.); aditiwagle05@gmail.com (A.W.); seongsuhui@naver.com (S.H.S.)
[2] Department of Food Science and Nutrition, Changshin University, Gyeongsangnam-do 51352, Korea;
    parkhj@cs.ac.kr
[3] Department of Food Science and Human Nutrition, Chonbuk National University, Jeonju 54896, Korea
*   Correspondence: jungha@jbnu.ac.kr (H.A.J.); choijs@pknu.ac.kr (J.S.C.);
    Tel.: +82-63-270-4882 (H.A.J.); +82-51-629-5845 (J.S.C.)

Abstract: A marine red alga, *Symphyocladia latiuscula* (Harvey) Yamada (Rhodomelaceae), is a rich source of bromophenols with a wide array of biological activities. This study investigates the anti-tyrosinase activity of the alga. Moderate activity was demonstrated by the methanol extract of *S. latiuscula*, and subsequent column chromatography identified three bromophenols: 2,3,6-tribromo-4,5-dihydroxybenzyl methyl alcohol (**1**), 2,3,6-tribromo-4,5-dihydroxybenzyl methyl ether (**2**), and bis-(2,3,6-tribromo-4,5-dihydroxybenzyl methyl ether) (**3**). Bromophenols **1** and **3** exhibited potent competitive tyrosinase inhibitory activity against L-tyrosine substrates, with IC_{50} values of 10.78 ± 0.19 and 2.92 ± 0.04 μM, respectively. Against substrate L-3,4-dihydroxyphenylalanine (L-DOPA), compounds **1** and **3** demonstrated moderate activity, while **2** showed no observable effect. The experimental data were verified by a molecular docking study that found catalytic hydrogen and halogen interactions were responsible for the activity. In addition, compounds **1** and **3** exhibited dose-dependent inhibitory effects in melanin and intracellular tyrosinase levels in α-melanocyte-stimulating hormone (α-MSH)-induced B16F10 melanoma cells. Compounds **3** and **1** were the most effective tyrosinase inhibitors. In addition, increasing the bromine group number increased the mushroom tyrosinase inhibitory activity.

Keywords: *Symphyocladia latiuscula*; bromophenols; mushroom tyrosinase; B16F10; melanin

1. Introduction

Marine algae are widely used in a variety of cuisines [1] and are preferred by a growing number of consumers for their functional and nutraceutical properties [2,3]. The pharmaceutical industry has also developed a strong interest in algae [4,5], as have cosmetologists [6]. A major concern among the latter is hyperpigmentation, which is an abnormal darkening of the skin associated with excessive melanin production [7,8]. Although melanin is a pigment responsible for the photo-protective effect of skin, overproduction may lead to skin disorders [9]. Because tyrosinase is a rate-limiting step in melanin formation, identification of a strong tyrosinase inhibitor would be of significant value to hyperpigmentation research.

Melanogenesis describes the production of distinct melanin pigments by specialized cells called melanocytes, which are found within membrane-bound organelles known as melanosomes [10]. The embryonic precursors of melanocytes, i.e., melanoblasts, originate in neural crest cells [11].

Mature melanocytes are connected with keratinocytes through dendritic cells, which facilitate the transfer of melanin in neighboring keratinocytes cells, are responsible for skin pigmentation, and protect the skin from harmful ultraviolet radiation [12]. Melanocyte-specific markers, which are used to identify the expression of melanocyte cells in the melanogenesis process, include tyrosinase, tyrosinase-related protein 1 (TRP1), tyrosinase-related protein 2 (TRP2)/dopachrome tautomerase (DCT), pre-melanosome protein 17 (Pmel17/gp100), melan-A/melanoma antigen recognized by T-cells 1 (MART-1), and microphthalmia-associated transcription factor (MITF). In melanin synthesis, the rate-limiting step is catalyzed by tyrosinase, while TRP1 is responsible for the oxidation of 5,6-dihydroxyindole-2-carboxylic acid to a carboxylated indole quinone [13]. Moreover, TRP2/DCT enzymes catalyze the tautomerization of dopachrome into 5,6-dihydroxyindole-2-carboxylic acid, which can be detected in both melanocytes and melanoblasts [14,15]. Pmel17/gp100 is necessary for the formation of the structural matrix of stage II melanosomes [16]. MART-1, meanwhile, is specifically targeted to tumor-directed T-lymphocytes and is a probable target for immunotherapy of melanoma [17]. MITF is a major transcriptional factor in the regulation of melanocyte-specific genes encoding tyrosinase, TRP2/DCT, and MART-1 [18–20].

Melanin pigments common in humans include eumelanin (a brown-black pigment) and pheomelanin (a yellow/orange-red pigment). Melanin is produced from its precursor, ʟ-tyrosine, through a series of enzymatic and chemical reactions. The first step of melanin biosynthesis, the oxidation of an ʟ-tyrosine substrate, is catalyzed by the rate-limiting enzyme tyrosinase. This is followed by dopaquinone formation [21,22]. Autoxidation of dopaquinone leads to the formation of ʟ-DOPA and dopachrome. ʟ-DOPA acts as a co-factor in the reaction [23] and also as a substrate for tyrosinase. Eumelanin is subsequently formed through a series of oxidation reactions with dihydroxyindole and dihydroxyindole-2-carboxylic acid. Dopaquinone is condensed into cysteinyldopa or glutathionyldopa in the presence of cysteine or gluthathione, producing pheomelanin pigments. A heterogeneous pool of mixed-type melanins can also be formed through interactions between eumelanin and pheomelanin [22,24].

Recently, marine algae have gained considerable interest in the discovery of tyrosinase inhibitors. In a study conducted to find new anti-browning and whitening agents from marine sources, Cha et al. [25] screened 43 indigenous marine algae for tyrosinase inhibitory activity and found potent tyrosinase inhibitory activity of extracts from *Endarachne binghamiae*, *Schizymenia dubyi*, *Ecklonia cava*, and *Sargassum silquastrum*. However, *Symphyocladia latiuscula* (Harvey) Yamada was not in the list of the 43 studied algae. Of the total microalgae in marine source, brown algae account for approximately 59%, followed by red algae at 40% and green algae at less than 1% [26], and phlorotannins and halogenated compounds are predominant secondary metabolites with prominent biological activities. Lately, tyrosinase inhibitory potentials of phlorotannins from marine algae have emerged with great interest [27–29]. Similarly, due to various advantages of halogens in drug pharmacokinetics such as lipophilicity, cell membrane solubility, membrane binding, permeation, diffusion, and half-life, chemists are focusing on the synthesis of novel tyrosinase inhibitors, taking halogenation as a basic tool [30–32]. However, reports on natural halogenated compounds from marine sources are limited. Therefore, this study focuses on a red alga, *Symphyocladia latiuscula*, and its constituent, bromophenols (Figure 1), for anti-tyrosinase activity.

Symphyocladia latiuscula (Harvey) Yamada is a member of the Rhodomelaceae family predominantly distributed along the coasts of Korea, Japan, and northern China. It is a red alga rich in bromophenols with a wide range of bioactive properties [33]. Among the compounds found in *S. latiuscula* are antioxidants [34,35], free radicals scavengers [36–38], peroxynitrite scavengers [39], anti-inflammatory and antibacterial [40], antifungal [41,42], antiviral [43], cytoprotective [39], and anti-diabetes [44], along with aldose reductase inhibitors [45], Taq DNA polymerase inhibitors [46], and anti-proliferators [47]. However, anti-tyrosinase activity has not yet been investigated in detail.
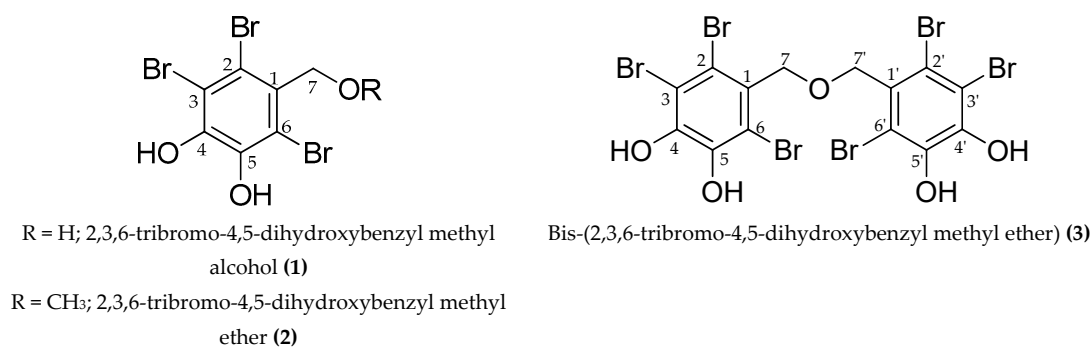
Figure 1. Structure of the compounds isolated from the ethyl acetate fraction of *S. latiuscula*.

2. Results

2.1. Effect of Bromophenols on Tyrosinase Activity

Mushroom tyrosinase inhibitory activity of MeOH extract of *S. latiuscula* demonstrated inhibition percentages of 39.58% and 86.47% at a concentration of 1000 and 250 μg/mL for L-tyrosine and L-DOPA, respectively. This result helped determine the compounds (Figure 1) responsible for the activity in the MeOH extract of *S. latiuscula*.

In L-tyrosine substrate, compound **3** demonstrated a potent mushroom tyrosinase inhibitory activity, with a half-maximal inhibitory concentration (IC_{50}) of 2.92 ± 0.04 μM, followed by compound **1** with 10.78 ± 0.04 μM. However, compound **2** exhibited weaker inhibition, with an IC_{50} value of 113.94 ± 0.75 μM (Table 1). Weak inhibition was also exhibited by compounds in L-DOPA substrate.

Table 1. Mushroom tyrosinase inhibitory potential of bromo-compounds from *S. latiuscula*.

Compounds	IC_{50} (μM) [a] (*n* = 3)		L-Tyrosine	
	L-Tyrosine	L-DOPA	K_i Value (μM) [b]	Inhibition Type [c]
1	10.78 ± 0.19 [h]	270.53 ± 2.04 [f]	10.59	Competitive
2	113.94 ± 0.75 [g]	>300	- [d]	- [d]
3	2.92 ± 0.04 [i]	110.91 ± 4.95 [g]	1.98	Competitive
Kojic acid [e]	3.17 ± 0.07 [i]	3.07 ± 0.04 [h]	- [d]	- [d]
Arbutin [e]	172.82 ± 4.71 [f]	>300	- [d]	- [d]

[a] The 50% inhibitory concentration (μM) expressed as mean ± SD of triplicate experiments; [b] The inhibition constant (K_i) was determined from secondary plots; [c] Inhibition type determined from Lineweaver-Burk plots; [d] Not determined; [e] Used as reference drug; [f–i] Means with different letters are significantly different with Duncan's test at $p < 0.05$.

2.2. Effect of Bromophenols on Enzyme Kinetic Inhibition

Changes in K_m values were observed on a double-reciprocal Lineweaver–Burk plot, which showed that compounds **1** and **3** induced competitive-type inhibition (Table 1, Figure 2). Furthermore, the secondary replot of K_{mapp}/V_{maxapp} and $1/V_{maxapp}$ versus compounds **1** and **3** was used to determine the binding constant of the inhibitor for free enzymes (K_{ic}). The K_{ic} ($\approx K_i$) values for compounds **1** and **3** were 10.59 and 1.98 μM.
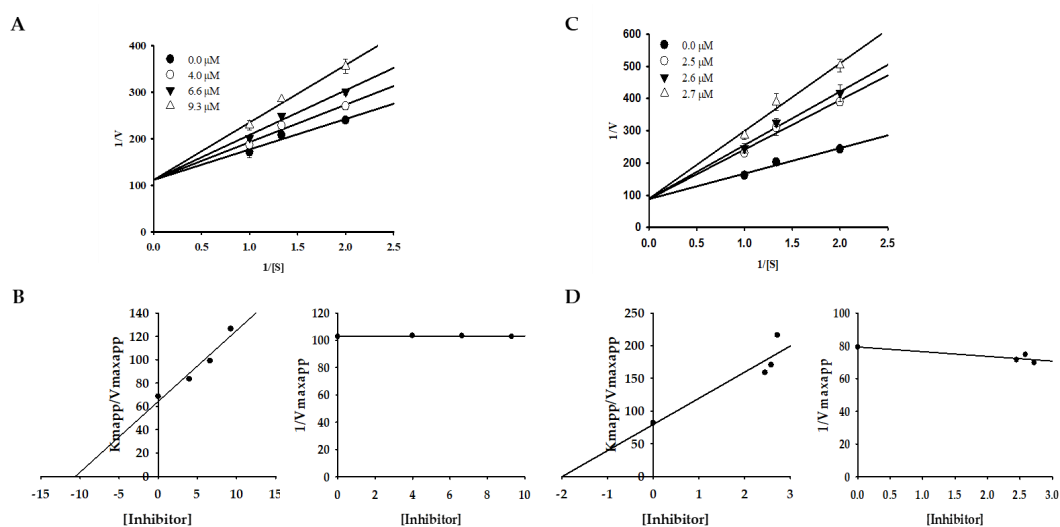
Figure 2. Lineweaver–Burk plots and the secondary plots of K_{mapp}/V_{maxapp} and $1/V_{maxapp}$ for the inhibition of tyrosinase by compounds **1** (**A**,**B**) and **3** (**C**,**D**) in the presence of different concentrations of substrate (L-tyrosine).

2.3. Molecular Docking Simulation on Tyrosinase Inhibition

To predict the binding site of the active compounds, a molecular docking simulation was performed. The binding energy, the number of hydrogen bonds, and the hydrogen-bond interaction, along with other interaction residues of the compounds and the reference compounds L-tyrosine (competitive inhibitor) and luteolin (allosteric inhibitor) are summarized in Table 2 and Figures 3 and 4. The most potent bromophenol, compound **3**, formed two hydrogen-bond interactions with Arg268 and peroxide ions (Per404) between the two copper ions. Furthermore, the complex was stabilized by His259, Asn260, Glu256, Met280, Val283, His263, Phe264, Ser282, Ala286, Val248, Met257, Val283, His85, His244, His259, His263, and Phe264 interacting residues (Figure 4C). Similarly, together with the three-hydrogen-bond interaction with Per404, Asn260, and His61, the compound **1**-tyrosinase complex was stabilized by Glu256, Met280, Val283, His263, Ala286, Val283, His85, Phe90, His244, His259, His263, and Phe264, as shown in Figure 4A. Likewise, only one hydrogen bond with peroxide ions was found with compound **2** (Figure 4B). The binding energies of −6.19, −6.29, and −7.81 kcal/mol were consumed by compounds **1**, **2**, and **3**, respectively.
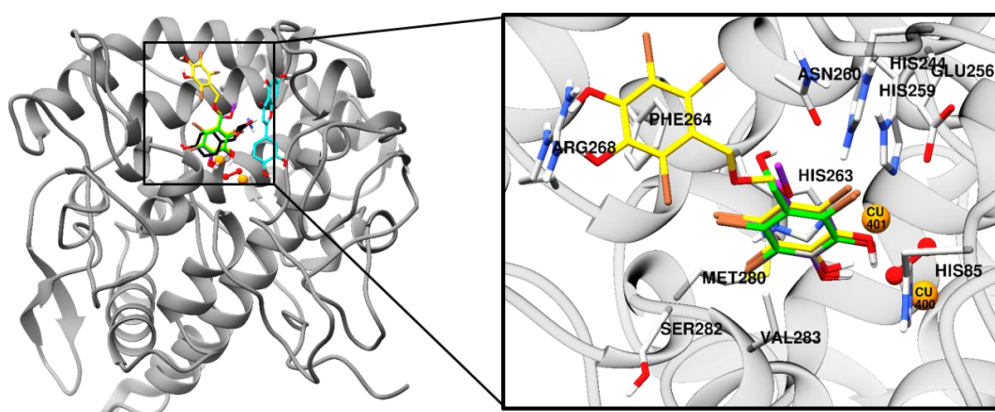
Figure 3. Molecular docking results of bromophenol compounds from *S. latiuscula* in the active site of oxy-form *Agaricus bisporus* tyrosinase (2Y9X) along with reference ligands. The chemical structure of compounds **1**, **2**, **3**, L-tyrosine, and luteolin are shown in green, purple, yellow, black, and cyan sticks, respectively. Bromine, oxygen, and nitrogen atoms are shown in brown, red, and blue, respectively. Copper and peroxide ions are shown in orange and red spheres, respectively.

Table 2. Binding energy and interacting residues of bromo-compounds from *S. latiuscula* against oxy-form *Agaricus bisporus* tyrosinase (2Y9X).

Compounds	Binding Energy (kcal/mol)	No. of H-Bonds	H-Bond Interactions	Other Interacting Residues
1	-6.19	3	Asn260, His61, and Per404 (O–H bond)	Glu256 and Met280 (O-Br bond), Val283 (Pi-Sigma), His263 (Pi-Pi Stacked), Ser282 (Amide-Pi Stacked), Ala286 and Val283 (Alkyl-Br), His85, Phe90, His244, His259, His263, and Phe264 (Pi-Br), Cu401, and 400 (van der Waals)
2	-6.29	1	Per404 (O–H bond)	Met280 (O-Br bond), Val283 (Pi-Sigma), His263 (Pi-Pi Stacked), Ala286 and Val283 (Alkyl-Br), His85, Phe90, His259, His263, and Phe264 (Pi-Br), Cu401, and 400 (van der Waals)
3	-7.81	2	Arg268 and Per404 (O–H bond)	His259 and Asn260 (C-O bond), Glu256 and Met280 (O-Br bond), Val283 (Pi-Sigma), His263 (Pi-Pi Stacked), Phe264 (Pi-Pi T-shaped), Ser282 (Amide-Pi Stacked), Ala286, Val248, Met257, and Val283 (Alkyl-Br), His85, His244, His259, His263, and Phe264 (Pi-Br), Cu401, and 400 (van der Waals)
L-Tyrosine [a]	-6.31	5	His244, Asn260, and Met280 (O–H bond), Glu256 (Salt-bridge)	Ala286 (Pi-Alkyl), Val283(Pi-Sigma), His263 (Pi-Pi Stacked), Cu401, and 400, Per402 (van der Waals)
Luteolin [a]	-5.77	4	Cys83, Gly245, Ala246, and Val248 (O–H bond)	Val248 (Pi-Alkyl), His85 (Pi-Sigma), Glu322 (Pi-Anion)

[a] L-tyrosine and luteolin were used as reference catalytic and allosteric inhibitor, respectively.
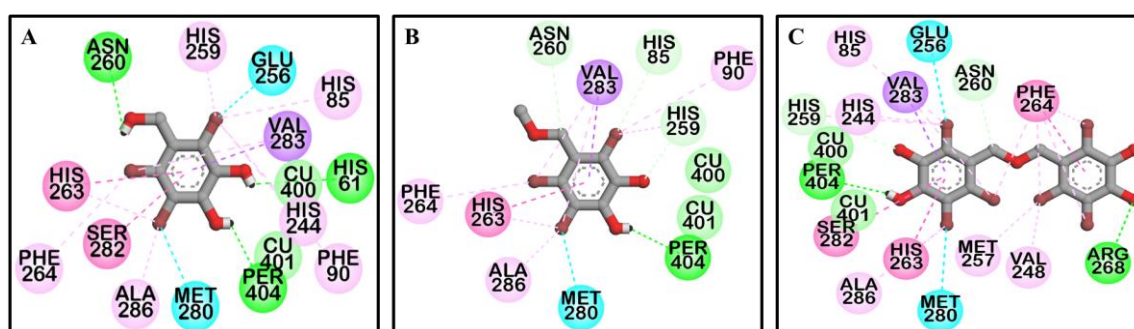
Figure 4. Molecular docking results of bromo-compounds **1** (**A**), **2** (**B**), and **3** (**C**) in the catalytic site of oxy-form *Agaricus bisporus* tyrosinase (2Y9X).

2.4. Effect of Bromophenols on Cell Viability of B16F10 Cells

To evaluate the toxicity of the bromophenols in B16F10 melanoma cells, cell viability upon bromophenol treatment only (Figure 5A) and/or co-treatment with 5 μM α-MSH for 48 h (Figure 5B) was determined using a 3-(4,5-dimethylthiazol-2-yl)-2,5-diphenyltetrazolium bromide (MTT) assay. The B16F10 melanoma cells were treated at a concentration of 25–100 μM of isolated bromophenols for 48 h. Bromophenol **2** showed no toxicity up to a concentration of 100 μM (approximately 100%

viable cells). However, compounds **1** and **3** displayed significant toxicity (74.6% and 86.9% viable cells, respectively). No toxicity was observed up to 50 μM concentration for all compounds. Consequently, a 25 μM sample concentration was used for further experiments.
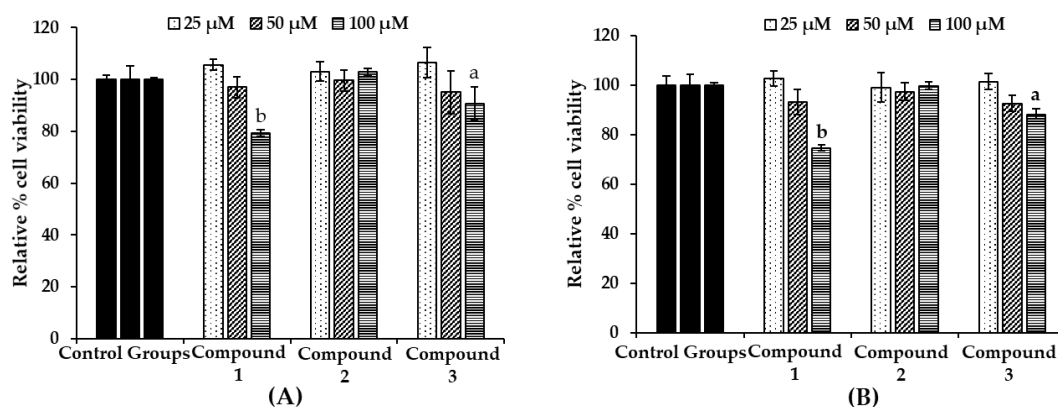
Figure 5. Effect of bromophenols **1**–**3** on cell viability in B16F10 cells (**A**) and co-treatment with 5 μM α-MSH (**B**). Cell viability was determined using the 3-(4,5-dimethylthiazol-2-yl)-2,5-diphenyl tetrazolium bromide (MTT) method. Cells were pretreated with the indicated concentrations (25, 50, and 100 μM) of test compounds for 48 h. Data shown represent mean ± SD of triplicate experiments. [a] $p < 0.05$ and [b] $p < 0.01$ indicates significant differences from the control group.

2.5. Effect of Bromophenols on Melanin Content and Intracellular Tyrosinase Activity in B16F10 Cells

Melanin and intracellular tyrosinase (TYR) contents were measured after pretreatment of B16F10 melanoma cells with different concentrations (6.25, 12.5, and 25 μM) of the three bromophenols for 1 h, followed by 48 h of α-MSH treatment. After stimulating B16F10 cells with 5 μM α-MSH for 48 h, the melanin content rose to 151.72% (Figure 6A). However, treatment of bromophenols **1** and **3** reduced the melanin content in a dose-dependent manner. At a 25 μM concentration, compounds **1** and **3** reduced the melanin content to 115.94% and 98.68%, respectively. Arbutin at a 500 μM concentration reduced the content to 124.06%. In parallel with the enzyme assay, compound **2** showed no significant reduction in the melanin content. Because cellular tyrosinase enhances melanin overproduction, reduction of tyrosinase activity is an efficient strategy for the development of anti-melanogenic agents. A L-DOPA oxidation protocol was designed to examine the inhibitory activity of isolated bromophenols against tyrosinase in α-MSH-induced B16F10 melanoma cells, because L-tyrosine and L-DOPA are sequentially generated substrates that regulate melanogenesis and modulate melanocyte function through overlapping substrates. After 48 h of sample treatment, intracellular tyrosinase activity was measured. As shown in Figure 6B, with treatments **1** and **3**, intracellular tyrosinase activity decreased in a dose-dependent manner compared with controls. The level of intracellular tyrosinase after α-MSH treatment was 215.73%, which was reduced to 122.64% and 94.81% after treatment with 25 μM concentration of **1** and **3**, respectively. The activities of **1** and **3** were better than that of 500 μM arbutin, which reduced intracellular tyrosinase levels to 130.75%. As with melanin content, compound **2** did not show a significant reduction in intracellular tyrosinase level at tested concentrations.
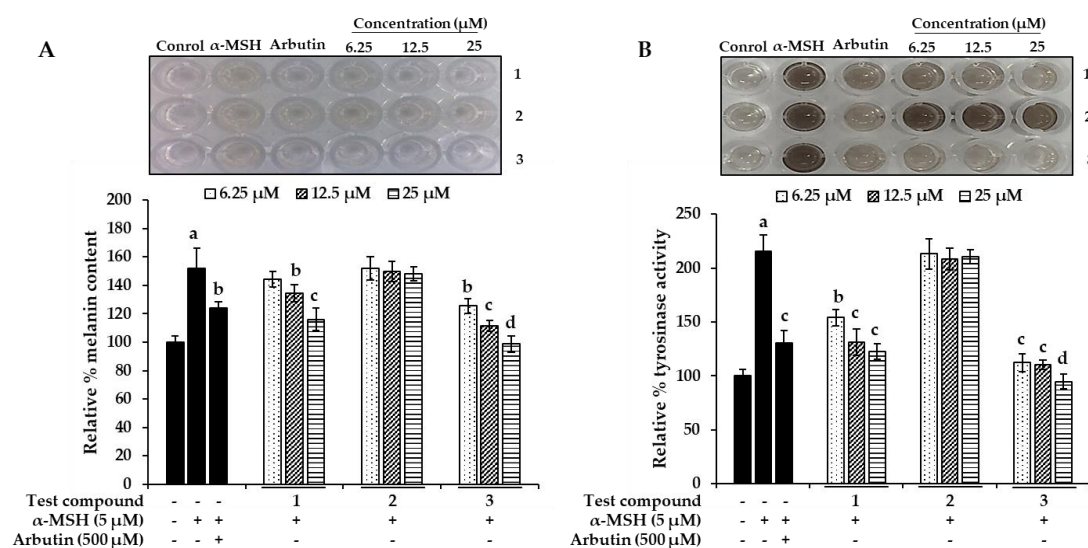
Figure 6. Effect of bromophenols **1**–**3** on extracellular melanin content (**A**) and cellular tyrosinase activity (**B**) in α-MSH-stimulated B16F10 cells. Cells were pretreated with the indicated concentrations (6.25, 12.5, and 25 μM) of bromophenols **1**–**3** for 1 h followed by exposure to α-MSH (5.0 μM) for 48 h in the presence or the absence of test bromophenols. Arbutin (500 μM) was used as a positive control. Values represent the mean ± SD of triplicate experiments. [a] $p < 0.01$ indicates significant differences from the control group; [b] $p < 0.05$, [c] $p < 0.01$ and [d] $p < 0.001$ indicate significant differences from the α-MSH treated group.

2.6. Effect of Bromophenols on Tyrosinase Expression

Increased tyrosinase activity enhances melanogenesis and hyperpigmentation, implying that downregulation of tyrosinase activity would theoretically represent an anti-pigmenting property. To evaluate the effect of bromophenols **1**-**3** on tyrosinase expression, the B16F10 cells were pre-treated with the bromophenols before stimulation with α-MSH, and the tyrosinase protein levels were examined using western blot analysis. As shown in Figure 7, treatment with compounds **1** and **3** at concentrations of 6.25, 12.5, and 25 μM for 48 h inhibited α-MSH-induced accumulation of tyrosinase proteins in a concentration-dependent manner.
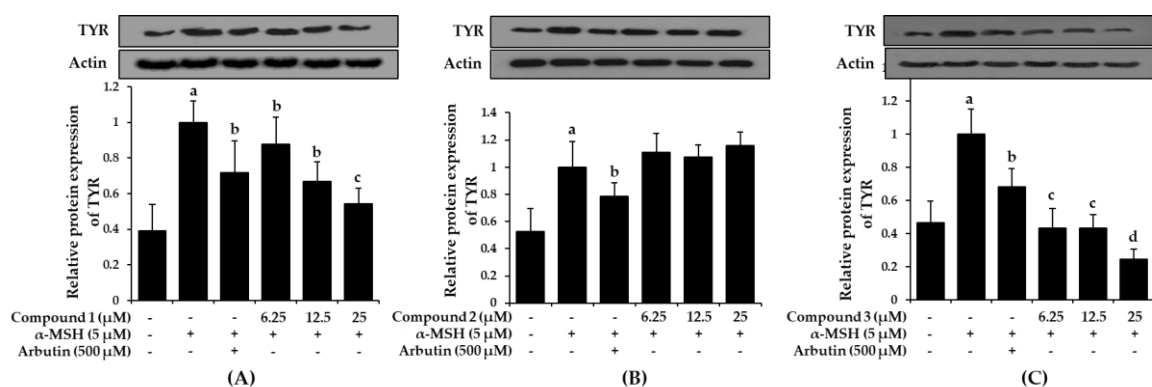
Figure 7. Effects of bromophenol **1** (**A**), **2** (**B**), and **3** (**C**) on cellular tyrosinase protein expression levels in α-MSH-stimulated B16F10 cells. Western blotting was performed, and protein band intensities were quantified by densitometric analysis. Upper panels display representative blots. Graphs under each bands represent the relative band density for tyrosinase (TYR) normalized to β-actin. Values represent the mean ± SD of three independent experiments; [a] $p < 0.001$ indicates significant differences from the control group; [b] $p < 0.05$, [c] $p < 0.01$ and [d] $p < 0.001$ indicate significant differences from the α-MSH treated group.

Compared with the normal control group, which had low levels of tyrosinase expression, the α-MSH-treated group demonstrated intensified tyrosinase expression levels. However, pre-treatment with arbutin and/or bromophenols **1** and **3** significantly reduced the expression levels. Compound **1** at 25 μM and compound **3** at 6.25 μM were more effective at downregulating tyrosinase expression than arbutin. Compound **2** did not reduce expression up to 25 μM.

3. Discussion

Use of cosmetics can lead to a variety of adverse effects and allergies in users sensitive to certain chemicals and other ingredients. To avoid unnecessary interactions and to reduce adverse effects of synthetic and semi-synthetic cosmetics, consumer preferences are shifting toward natural products. Marine species are an abundant source of chemical and bioactive compounds due to the variety of biological activities associated with marine organisms [48]. Many compounds derived from marine species with possible applications in the nutraceutical and cosmetics fields remain unexamined [49,50].

To meet the demand for new compounds that exhibit potent anti-tyrosinase activity, a preliminary screening of the methanolic extract of *S. latiuscula* was performed. The study revealed that a MeOH extract was associated with inhibition rates of 39.58% and 86.47% at concentrations of 1000 and 250 μg/mL for L-tyrosine and L-DOPA, respectively. A study performed by Seo and Yoo [51] reported inhibition rates of 84% and 60% against MeOH extract and a mixture of acetone and methylene chloride, respectively, using L-tyrosine as a substrate. In contrast, no inhibition was observed at a concentration of 500 μg/mL [27]. The possible reasons for the discrepancies among these experiments include the difference in concentrations of enzyme and substrate, incubation time, and environmental conditions. Based on the results, *S. latiuscula* extract was subjected to bio-assay guided fractionation, which yielded 2,3,6-tribromo-4,5-dihydroxybenzyl methyl alcohol (**1**), 2,3,6-tribromo-4,5-dihydroxybenzyl methyl ether (**2**), and bis-(2,3,6-tribromo-4,5-dihydroxybenzyl methyl ether) (**3**). For the first time, a mushroom tyrosinase inhibitory assay with an L-tyrosine substrate for the isolated compounds revealed compound **3** to be approximately twice and 23 times more potent than compounds **1** and **2**, respectively (Table 1). A similar tendency was observed for the L-DOPA substrate but with only moderate potency. This result highlights the dimeric form of compound **2**, specifically how the *O*-linkage of the 2,3,6-tribromo-4,5-dihydroxyl methyl ether element enhances mushroom tyrosinase inhibition. Moreover, an increased number for bromophenol moiety contributes to increased inhibition toward tyrosinase. The results were further verified by the observations of B16F10 melanoma cells, which had concentration-dependent inhibitory effects on melanin content and tyrosinase activity for compounds **1** and **3**. A similar tendency for reduction of tyrosinase expression levels by **1** and **3** was observed in a western blot analysis.

To shed light on the inhibition mode against tyrosinase, kinetic analysis for active compounds **1** and **3** using an L-tyrosine substrate was performed, supplemented by a molecular docking study. A double-reciprocal Lineweaver-Burk plot of compounds **1** and **3** for the oxidation of different concentrations of L-tyrosine demonstrated competitive inhibition of both compounds, as K_m changed while V_{max} was constant. Graphing 1/V versus 1/[S] produced a family of straight lines with diverse slopes, although the lines intersected on the *Y*-axis. The results showed that compounds **1** and **3** could only bind with free enzymes. An inhibition constant for the inhibitor binding with the free enzyme (K_{ic}) was obtained from the secondary plot as 10.59 and 1.98 μM.

To predict binding affinity, activity of the small molecules, and the interaction of the molecules, and to determine the optimal orientation of the protein–ligand complex with minimum energy, molecular docking tools can be applied. This helps reveal the underlying mechanism of the compound responsible for a particular bioactivity. A simulated docking study of the binding of the compounds to the catalytic site of tyrosinase (Figures 3 and 4) provided evidence of the competitive inhibition, as shown by a kinetic analysis (Figure 3). An H-bond interaction was formed by compound **1** as the fourth and fifth hydroxyl group interacted with the peroxide ion located between the two copper ions and His61, respectively, and the seventh hydroxyl group interacted with an Asn260 amino-acid

residue. Moreover, the O-atom at the carboxylic moiety of Glu256 and Met280 interacted with the third- and the sixth-position bromine atoms. The complex was stabilized by hydrophobic interactions with Val283, His263, and Ser282 and halogen interactions with Ala286, Val283, His85, Phe90, His244, His259, His263, and Phe264 residues (Figure 4A). Although similar interactions were observed for compound **3**, the strong H-bond interaction between Arg268 residue and the 4′-OH group of active compound **3** helped stabilize the compound **3**-tyrosinase complex [52]. Because of the increase in the bromine moiety number, there was an increase in halogen interactions assisting the potent anti-tyrosinase activity (Figure 4C). A similar result was seen in tyrosine phosphatase 1B and α-glucosidase inhibition [44]. Although compound **2** lacked the H-bond interaction with the other amino-acid residues, a peroxide ion between the two copper atoms can explain its weak tyrosinase inhibitory activity (Figure 4B). The lower the value of binding energy shown by the compounds was, the more stable the complex formed between the ligand and targeted protein was. Binding energies of compounds **1–3** to tyrosinase was comparable. However, compound **2** showed ineffective anti-melanogenic activity. The probable reason for this discrepancy might be that, despite the fact that compound **2** was involved in van der Waals interactions with copper ions (Cu401 and 400) and H-bond interactions with a peroxide ion (Per404) at the active site, the complex was not stable. For **1** and **3**, H-bond interactions with Asn260 and Arg268 and hydrophobic interaction with Ser282 most probably stabilized the complex, and these interactions were not observed for **2**. However, this should be confirmed through molecular dynamic simulation. Moreover, as the present study reports just three compounds, the structural-activity relationship study might be incomplete. Therefore, in depth study of the structural-activity relationship with a larger number of bromophenols is warranted. The results confirm the strong activity exhibited by the compounds isolated from *S. latiuscula,* making the alga a possible source for depigmenting agents in cosmetology.

4. Materials and Methods

4.1. Chemicals and Reagents

L-Tyrosine, L-3,4-dihydroxyphenylalanine (L-DOPA), arbutin, mushroom tyrosinase enzyme (EC 1.14.18.1), and α-melanocyte-stimulating hormone (α-MSH) were obtained from Sigma Aldrich (St. Louis, MO, USA). Dulbecco's modified Eagle's medium (DMEM), fetal bovine serum (FBS), and penicillin-streptomycin were purchased from Gibco-BRL Life Technologies (Grand Island, NY, USA). Primary tyrosinase (TYR) antibodies, β-actin, and horseradish peroxidase-conjugated secondary antibodies were obtained from Santa Cruz Biotechnology Inc. (Santa Cruz, CA, USA). Dipotassium phosphate and monopotassium phosphate were obtained from Junsei Chemical Co. Ltd. (Tokyo, Japan) and Yakuri Pure Chemicals Co. Ltd. (Osaka, Japan), respectively. All other reagents and solvents were purchased from E. Merck, Fluka, and Sigma-Aldrich unless otherwise stated.

4.2. Algal Material

Leafy thalli of *S. latiuscula* (Harvey) Yamada collected from Cheongsapo, Busan, Korea, in January 2016 were authenticated by an algologist, Doctor K. W. Nam, at the Department of Marine Biology, Pukyong National University. A voucher specimen (No. 20160140) was deposited in the laboratory of professor J. S. Choi, Pukyong National University.

4.3. Extraction, Fractionation, and Isolation

Clean and dried leafy thalli of *S. latiuscula* (Harvey) Yamada (700 g) was extracted in methanol (MeOH) three times successively for 3 h at a time (5 L × 3 times) under reflux, followed by concentration until dry in vacuo at 40 °C to obtain 207.38 g of MeOH extract. The resulting MeOH extract was successively partitioned with different solvent soluble fractions. Details on partition, isolation, and identification of compounds are reported in Paudel et al. [44].

4.4. Mushroom Tyrosinase Inhibitory Assay

The inhibitory activity of mushroom tyrosinase was carried out using a spectrophotometric method described in [27] with slight modifications. In brief, 10 μL of samples/positive control (kojic acid) together with 50 mM of phosphate buffer (pH 6.5), 1 mM of substrate (L-tyrosine/L-DOPA) solution, and distilled water were mixed at a ratio of 10:10:9 in a 96-well plate. Then, 20 μL of tyrosinase was added and incubated at room temperature for between 10 and 30 minutes. Absorbance was measured at 490 nm after incubation.

4.5. Kinetic Study Against Mushroom Tyrosinase

The inhibition type was determined using a Lineweaver–Burk plot [53]. The apparent slope (K_{mapp}/V_{maxapp}) and intercept ($1/V_{maxapp}$) versus different inhibitor concentrations was used to determine the inhibition constant (K_i) [54]. Different kinetic parameters were obtained for different concentrations of the substrate (0.5, 0.75, and 1 mM) and inhibitors (compound **1**—0.0, 4.0, 6.6, and 9.3 μM; compound **3**—0, 2.5, 2.6, and 2.7 μM). Sigmaplot version 12.0 (SPSS Inc., Chicago, IL, USA) was employed to generate the plots.

4.6. Molecular Docking Simulation of Mushroom Tyrosinase

Molecular docking analysis was carried out using the procedure described [55] in AutoDock 4.2. Structures for L-tyrosine (6057) and luteolin (5280445) were obtained from the PubChem compound database. The three-dimensional (3D) structures of the bromophenol compounds were generated by Marvin Sketch (v17.1.30, ChemAxon, Budapest, Hungary). Docking results were visualized and analyzed using PyMOL (v1.7.4, Schrödinger, LLC, Cambridge, MA) and Discovery Studio (v16.1, Accelrys, San Diego, CA, USA).

4.7. Cell Culture and Viability Assay

B16F10 mouse melanoma cells obtained from American Type Culture Collection (Manassas, VA, USA) were maintained in 10% FBS in high-glucose DMEM containing 100 U/mL penicillin and 100 μg/mL streptomycin at 37 °C in a humidified atmosphere with 5% CO_2. Cytotoxicity was evaluated using a 3-(4,5-dimethylthiazol-2-yl)-2,5-diphenyltetrazolium bromide (MTT) assay. After 95% of confluence, B16F10 cells were seeded in a 96-well plate at 10,000 cells/well and incubated for 24 h in DMEM supplemented with 10% FBS. The cells were then fed fresh serum-free DMEM containing different concentrations (25 to 100 μM) of the test compounds and incubated for 48 h. After that, the cells were incubated with 100 μL of MTT at a concentration of 0.5 μg/mL in phosphate-buffered saline (PBS) for 2 h. Absorbance was measured at 490 nm by a microplate reader (Promega Corporation Instrument, USA) after 2 h of incubation. The viability of cells at 48 h upon co-treatment with α-MSH was evaluated by treating cells with 5 μM α-MSH 1 h after the treatment with test compounds.

4.8. Melanin Content Assay

Intracellular melanin content was determined according to a previously reported procedure [56] with minor modifications. Briefly, B16F10 cells were seeded in a 24-well plate at $2 \times 10,000$ cells/well and incubated for 24 h in DMEM containing 10% FBS. Cells were pretreated with 6.25, 12.5, and 25 μM test compounds for 1 h and stimulated with 5 μM α-MSH for 48 h. Arbutin (500 μM) was used as a positive control. The cells were washed with PBS and dissolved in 1 N NaOH containing 10% DMSO by boiling at 80 °C for 30 min. The cell lysates were centrifuged at 14,000 rpm for 20 min, and absorbance of the supernatant was measured at 405 nm. Melanin content was determined by normalizing the absorbance with total protein content.

4.9. Cellular Tyrosinase Assay

Intracellular tyrosinase inhibitory activity was evaluated by measuring the rate of oxidation of ʟ-DOPA [57]. Briefly, $2 \times 10,000$ cells/well were seeded and incubated for 24 h in a 6-well plate and treated with various concentrations of bromophenols (6.25, 12.5, and 25 μM) or arbutin (500 μM) for 1 h, then stimulated with α-MSH (5 μM) for 48 h. The cells were washed with PBS and lysed with a radio immunoprecipitation assay buffer. The cell lysates were kept in a deep freezer ($-80\ °C$) for 1 h. After defrosting the cell lysates, the cellular extracts were purified by centrifugation at 14,000 rpm for 20 min at 4 °C, and the supernatant was used as cellular tyrosinase solution. A total of 80 μL of supernatant and 20 μL of ʟ-DOPA (2 mg/mL) were added to a 96-well plate and incubated at 37 °C for 45 min. Dopachrome formation was then measured spectrophotometrically at 450 nm using a microplate spectrophotometer (Molecular Devices). Intracellular tyrosinase activity was calculated as the percentage of control.

4.10. Determination of Tyrosinase Protein Levels via Western Blotting

After stimulating B16F10 cells with α-MSH in the presence or the absence of test bromophenols and arbutin for the indicated times, the cells were washed with ice-cold PBS and harvested using a cell scraper. The cell suspensions were centrifuged at $16,000 \times g$ for 5 min, and the cell pellets were lysed in a lysis buffer and incubated on ice for 10 min. The cell lysates were centrifuged at $16,000 \times g$ for 10 min, and the supernatant (total protein) was normalized using a Bradford protein assay kit. Aliquots of protein were resolved by sodium dodecyl sulfate-polyacrylamide gel electrophoresis and transferred onto a nitrocellulose membrane. The membrane was blocked with 10% nonfat milk (*w/v*) in tris-buffered saline with tween (TBST) (0.1 M Tris-HCl, pH 7.5, 1.5 M NaCl, 1% Tween20) for 2 h and incubated for approximately 24 h with TYR primary antibody. The immunoblots were then incubated with appropriate secondary antibodies for 2 h and detected using an enhanced chemiluminescence detection kit.

4.11. Statistical Analysis

One-way ANOVA and a Student's *t*-test (Systat Inc., Evanston, IL, USA) were used to determine statistical significance. Values of $p < 0.05, 0.01, 0.001$, and 0.0001 were considered significant. All results are presented as the mean ± SD of triplicate experiments.

5. Conclusions

The present study revealed that, among three bromophenols isolated from the marine alga *S. latiuscula*, compound **3** followed by **1** exhibited potent competitive tyrosinase inhibition against ʟ-tyrosine substrate. A molecular docking simulation of the catalytic residue revealed the underlying inhibitory mechanism. In addition, compounds **1** and **3** inhibited cellular tyrosinase activity, decreased tyrosinase protein expression levels, and reduced the melanin content in α-MSH-treated B16F10 melanoma cells in a concentration-dependent manner. These results suggest that the increased number of bromine groups in the compound is associated with significant mushroom tyrosinase inhibitory activity. Overall, the strong tyrosinase inhibitory activity exhibited by the bromophenols isolated from *S. latiuscula* makes the alga a possible source for depigmenting agents in cosmetology.

Author Contributions: P.P. participated in study design, isolation, cell-based assays, and wrote some part and revised the manuscript. A.W. performed enzyme assays and drafted the manuscript. S.H.S. performed the molecular docking studies and wrote part of manuscript. H.J.P. collected plant material. H.A.J. was involved in spectral analysis, statistical analysis and wrote part of the manuscript. J.S.C. conceived the study, coordinated the study and interpreted the data. All authors read and approved the final manuscript.

Conflicts of Interest: The authors declare no conflict of interest.

References

1. Rajapakse, N.; Kim, S.K. Nutritional and digestive health benefits of seaweed. In *Advances in Food and Nutrition Research*; Kim, S.-K., Ed.; Elsevier: San Diego, CA, USA, 2011; Volume 64, pp. 17–28.

2. Suleria, H.; Osborne, S.; Masci, P.; Gobe, G. Marine-based nutraceuticals: An innovative trend in the food and supplement industries. *Mar. Drugs* **2015**, *13*, 6336–6351. [CrossRef]

3. Wells, M.L.; Potin, P.; Craigie, J.S.; Raven, J.A.; Merchant, S.S.; Helliwell, K.E.; Smith, A.G.; Camire, M.E.; Brawley, S.H. Algae as nutritional and functional food sources: Revisiting our understanding. *J. Appl. Phycol.* **2017**, *29*, 949–982. [CrossRef]

4. Jeon, Y.J.; Samarakoon, K.W.; Elvitigala, D.A. Marine-derived pharmaceuticals and future prospects. In *Springer Handbook of Marine Biotechnology*; Springer-Verlag Berlin Heidelberg: Berlin, Germany, 2015; pp. 957–968.

5. Siahaan, E.A.; Pangestuti, R.; Kim, S.K. Seaweeds: Valuable ingredients for the pharmaceutical industries. In *Grand Challenges in Marine Biotechnology*; Springer International Publishing AG: Cham, Switzerland, 2018; pp. 49–95.

6. Thomas, N.; Kim, S.K. Beneficial effects of marine algal compounds in cosmeceuticals. *Mar. Drugs* **2013**, *11*, 146–164. [CrossRef]

7. Lerner, A.B.; Fitzpatrick, T.B. Treatment of melanin hyperpigmentation. *JAMA* **1953**, *152*, 577–582. [CrossRef]

8. Rigopoulos, D.; Gregoriou, S.; Katsambas, A. Hyperpigmentation and melasma. *J. Cosmet. Dermatol.* **2007**, *6*, 195–202. [CrossRef]

9. Brown, D.A. Skin pigmentation enhancers. In *Comprehensive Series in Photosciences*; Elsevier Science: Amsterdam, The Netherlands, 2001; Volume 3, pp. 637–675.

10. Costin, G.E.; Hearing, V.J. Human skin pigmentation: Melanocytes modulate skin color in response to stress. *FASEB J.* **2007**, *21*, 976–994. [CrossRef]

11. Cichorek, M.; Wachulska, M.; Stasiewicz, A.; Tymińska, A. Skin melanocytes: Biology and development. *Postepy. Dermatol. Alergol.* **2013**, *30*, 30. [CrossRef]

12. Tsatmali, M.; Ancans, J.; Thody, A.J. Melanocyte function and its control by melanocortin peptides. *J. Histochem. Cytochem.* **2002**, *50*, 125–133. [CrossRef]

13. Kobayashi, T.; Urabe, K.; Winder, A.; Jiménez-Cervantes, C.; Imokawa, G.; Brewington, T.; Solano, F.; García-Borrón, J.; Hearing, V. Tyrosinase related protein 1 (TRP1) functions as a DHICA oxidase in melanin biosynthesis. *EMBO J.* **1994**, *13*, 5818–5825. [CrossRef]

14. Körner, A.M.; Pawelek, J. Dopachrome conversion: A possible control point in melanin biosynthesis. *J. Invest. Dermatol.* **1980**, *75*, 192–195. [CrossRef]

15. Steel, K.; Davidson, D.R.; Jackson, I. TRP-2/DT, a new early melanoblast marker, shows that steel growth factor (c-kit ligand) is a survival factor. *Development* **1992**, *115*, 1111–1119. [PubMed]

16. Valencia, J.C.; Watabe, H.; Chi, A.; Rouzaud, F.; Chen, K.G.; Vieira, W.D.; Takahashi, K.; Yamaguchi, Y.; Berens, W.; Nagashima, K. Sorting of Pmel17 to melanosomes through the plasma membrane by AP1 and AP2: Evidence for the polarized nature of melanocytes. *J. Cell Sci.* **2006**, *119*, 1080–1091. [CrossRef]

17. Kawakami, Y.; Robbins, P.F.; Wang, R.F.; Parkhurst, M.; Kang, X.; Rosenberg, S.A. The use of melanosomal proteins in the immunotherapy of melanoma. *J. Immunother.* **1998**, *21*, 237–246. [CrossRef]

18. Bertolotto, C.; Abbe, P.; Hemesath, T.J.; Bille, K.; Fisher, D.E.; Ortonne, J.P.; Ballotti, R. Microphthalmia gene product as a signal transducer in cAMP-induced differentiation of melanocytes. *J. Cell Biol.* **1998**, *142*, 827–835. [CrossRef]

19. Levy, C.; Khaled, M.; Fisher, D.E. MITF: Master regulator of melanocyte development and melanoma oncogene. *Trends Mol. Med.* **2006**, *12*, 406–414. [CrossRef]

20. Shibahara, S.; Yasumoto, K.I.; Amae, S.; Udono, T.; Watanabe, K.I.; Saito, H.; Takeda, K. Regulation of pigment cell-specific gene expression by MITF. *Pigment Cell Res.* **2000**, *13*, 98–102. [CrossRef]

21. Fitzpatrick, T.B.; Becker, S.W.; Lerner, A.B.; Montgomery, H. Tyrosinase in human skin: Demonstration of its presence and of its role in human melanin formation. *Science* **1950**, *112*, 223–225. [CrossRef]

22. Ortonne, J.P. Photoprotective properties of skin melanin. *Br. J. Dermatol.* **2002**, *146*, 7–10. [CrossRef]

23. Pomerantz, S.H.; Warner, M.C. 3,4-Dihydroxy-L-phenylalanine as the tyrosinase cofactor occurrence in melanoma and binding constant. *J. Biol. Chem.* **1967**, *242*, 5308–5314. [PubMed]

24. Riley, P. Melanin. *Int. J. Biochem. Cell Biol.* **1997**, *29*, 1235–1239. [CrossRef]

25. Cha, S.H.; Ko, S.C.; Kim, D.; Jeon, Y.J. Screening of marine algae for potential tyrosinase inhibitor: Those inhibitors reduced tyrosinase activity and melanin synthesis in zebrafish. *J. Dermatol.* **2011**, *38*, 354–363. [CrossRef]

26. Wang, H.M.D.; Chen, C.C.; Huynh, P.; Chang, J.S. Exploring the potential of using algae in cosmetics. *Bioresour. Technol.* **2015**, *184*, 355–362. [CrossRef] [PubMed]

27. Kang, H.S.; Kim, H.R.; Byun, D.S.; Son, B.W.; Nam, T.J.; Choi, J.S. Tyrosinase inhibitors isolated from the edible brown alga *Ecklonia stolonifera*. *Arch. Pharm. Res.* **2004**, *27*, 1226–1232. [CrossRef] [PubMed]

28. Yoon, N.Y.; Eom, T.K.; Kim, M.M.; Kim, S.K. Inhibitory effect of phlorotannins isolated from *Ecklonia cava* on mushroom tyrosinase activity and melanin formation in mouse B16F10 melanoma cells. *J. Agric. Food Chem.* **2009**, *57*, 4124–4129. [CrossRef] [PubMed]

29. Heo, S.J.; Ko, S.C.; Cha, S.H.; Kang, D.H.; Park, H.S.; Choi, Y.U.; Kim, D.; Jung, W.K.; Jeon, Y.J. Effect of phlorotannins isolated from *Ecklonia cava* on melanogenesis and their protective effect against photo-oxidative stress induced by UV-B radiation. *Toxicol. In Vitro* **2009**, *23*, 1123–1130. [CrossRef]

30. Matos, M.J.; Santana, L.; Uriarte, E.; Delogu, G.; Corda, M.; Fadda, M.B.; Era, B.; Fais, A. New halogenated phenylcoumarins as tyrosinase inhibitors. *Bioorg. Med. Chem. Lett.* **2011**, *21*, 3342–3345. [CrossRef]

31. Ismail, T.; Shafi, S.; Srinivas, J.; Sarkar, D.; Qurishi, Y.; Khazir, J.; Alam, M.S.; Kumar, H.M.S. Synthesis and tyrosinase inhibition activity of trans-stilbene derivatives. *Bioorg. Chem.* **2016**, *64*, 97–102. [CrossRef] [PubMed]

32. Onul, N.; Ertik, O.; Mermer, N.; Yanardag, R. Synthesis and biological evaluation of S-substituted perhalo-2-nitrobuta-1,3-dienes as novel xanthine oxidase, tyrosinase, elastase, and neuraminidase inhibitors. *J. Chem.* **2018**, *2018*. [CrossRef]

33. Xu, X.; Yang, H.; Khalil, Z.; Yin, L.; Xiao, X.; Neupane, P.; Bernhardt, P.; Salim, A.; Song, F.; Capon, R. Chemical diversity from a Chinese marine red alga, *Symphyocladia latiuscula*. *Mar. Drugs* **2017**, *15*, 374. [CrossRef] [PubMed]

34. Huang, H.L.; Wang, B.G. Antioxidant capacity and lipophilic content of seaweeds collected from the Qingdao coastline. *J. Agric. Food Chem.* **2004**, *52*, 4993–4997. [CrossRef]

35. Kang, H.S.; Chung, H.Y.; Kim, J.Y.; Son, B.W.; Jung, H.A.; Choi, J.S. Inhibitory phlorotannins from the edible brown alga *Ecklonia stolonifera* on total reactive oxygen species (ROS) generation. *Arch. Pharm. Res.* **2004**, *27*, 194–198. [CrossRef]

36. Choi, J.S.; Park, H.J.; Jung, H.A.; Chung, H.Y.; Jung, J.H.; Choi, W.C. A cyclohexanonyl bromophenol from the red alga *Symphyocladia latiuscula*. *J. Nat. Prod.* **2000**, *63*, 1705–1706. [CrossRef] [PubMed]

37. Duan, X.J.; Li, X.M.; Wang, B.G. Highly brominated mono-and bis-phenols from the marine red alga *Symphyocladia latiuscula* with radical-scavenging activity. *J. Nat. Prod.* **2007**, *70*, 1210–1213. [CrossRef] [PubMed]

38. Xu, X.; Yin, L.; Gao, L.; Gao, J.; Chen, J.; Li, J.; Song, F. Two new bromophenols with radical scavenging activity from marine red alga *Symphyocladia latiuscula*. *Mar. Drugs* **2013**, *11*, 842–847. [CrossRef] [PubMed]

39. Chung, H.Y.; Choi, H.R.; Park, H.J.; Choi, J.S.; Choi, W.C. Peroxynitrite scavenging and cytoprotective activity of 2,3,6-tribromo-4,5-dihydroxybenzyl methyl ether from the marine alga *Symphyocladia latiuscula*. *J. Agric. Food Chem.* **2001**, *49*, 3614–3621. [CrossRef]

40. Choi, J.S.; Bae, H.J.; Kim, S.J.; Choi, I.S. In vitro antibacterial and anti-inflammatory properties of seaweed extracts against acne inducing bacteria, *Propionibacterium acnes*. *J. Environ. Biol.* **2011**, *32*, 313.

41. Xu, X.; Yin, L.; Wang, Y.; Wang, S.; Song, F. A new bromobenzyl methyl sulphoxide from marine red alga *Symphyocladia latiuscula*. *Nat. Prod. Res.* **2013**, *27*, 723–726. [CrossRef]

42. Xu, X.; Yin, L.; Gao, J.; Gao, L.; Song, F. Antifungal bromophenols from marine red alga *Symphyocladia latiuscula*. *Chem. Biodivers.* **2014**, *11*, 807–811. [CrossRef]

43. Park, H.J.; Kurokawa, M.; Shiraki, K.; Nakamura, N.; Choi, J.S.; Hattori, M. Antiviral activity of the marine alga *Symphyocladia latiuscula* against herpes simplex virus (HSV-1) in vitro and its therapeutic efficacy against HSV-1 infection in mice. *Biol. Pharm. Bull.* **2005**, *28*, 2258–2262. [CrossRef]

44. Paudel, P.; Seong, S.H.; Park, H.J.; Jung, H.A.; Choi, J.S. Anti-diabetic activity of 2,3,6-tribromo-4,5-dihydroxybenzyl derivatives from *Symphyocladia latiuscula* through PTP1B downregulation and α-glucosidase inhibition. *Mar. Drugs* **2019**, *17*, 166. [CrossRef]

45. Wang, W.; Okada, Y.; Shi, H.; Wang, Y.; Okuyama, T. Structures and aldose reductase inhibitory effects of bromophenols from the red alga *Symphyocladia latiuscula*. *J. Nat. Prod.* **2005**, *68*, 620–622. [CrossRef]

46. Jin, H.J.; Oh, M.Y.; Jin, D.H.; Hong, Y.K. Identification of a Taq DNA polymerase inhibitor from the red seaweed *Symphyocladia latiuscula*. *J. Environ. Biol.* **2008**, *29*, 475–478.

47. Lee, J.H.; Park, S.E.; Hossain, M.A.; Kim, M.Y.; Kim, M.N.; Chung, H.Y.; Choi, J.S.; Yoo, Y.H.; Kim, N.D. 2,3,6-Tribromo-4,5-dihydroxybenzyl methyl ether induces growth inhibition and apoptosis in MCF-7 human breast cancer cells. *Arch. Pharm. Res.* **2007**, *30*, 1132–1137. [CrossRef] [PubMed]

48. De Vries, D.J.; Beart, P.M. Fishing for drugs from the sea: Status and strategies. *Trends Pharmacol. Sci.* **1995**, *16*, 275–279. [CrossRef]

49. Guillerme, J.B.; Couteau, C.; Coiffard, L. Applications for marine resources in cosmetics. *Cosmetics* **2017**, *4*, 35. [CrossRef]

50. Kim, S.K. Marine cosmeceuticals. *J. Cosmet. Dermatol.* **2014**, *13*, 56–67. [CrossRef] [PubMed]

51. Seo, Y.W.; Yoo, J.S. Screening for antioxidizing and tyrosinase-inhibitory activities of the extracts of marine algae from Busan coastal area. *Ocean Polar Res.* **2003**, *25*, 129–132. [CrossRef]

52. Wagle, A.; Seong, S.H.; Joung, E.J.; Kim, H.R.; Jung, H.A.; Choi, J.S. Discovery of a highly potent tyrosinase inhibitor, luteolin 5-*O*-β-ᴅ-glucopyranoside, isolated from *Cirsium japonicum* var. *maackii* (Maxim.) Matsum., Korean thistle: Kinetics and computational molecular docking simulation. *ACS Omega* **2018**, *3*, 17236–17245.

53. Lineweaver, H.; Burk, D. The determination of enzyme dissociation constants. *J. Am. Chem. Soc.* **1934**, *56*, 658–666. [CrossRef]

54. Kim, J.H.; Morgan, A.M.; Tai, B.H.; Van, D.T.; Cuong, N.M.; Kim, Y.H. Inhibition of soluble epoxide hydrolase activity by compounds isolated from the aerial parts of *Glycosmis stenocarpa*. *J. Enzyme Inhib. Med. Chem.* **2016**, *31*, 640–644. [CrossRef]

55. Wagle, A.; Seong, S.H.; Jung, H.A.; Choi, J.S. Identifying an isoflavone from the root of *Pueraria lobata* as a potent tyrosinase inhibitor. *Food Chem.* **2019**, *276*, 383–389. [CrossRef] [PubMed]

56. Azam, M.S.; Kwon, M.; Choi, J.; Kim, H.R. Sargaquinoic acid ameliorates hyperpigmentation through cAMP and ERK-mediated downregulation of MITF in α-MSH-stimulated B16F10 cells. *Biomed. Pharmacother.* **2018**, *104*, 582–589. [CrossRef] [PubMed]

57. Bae, S.J.; Ha, Y.M.; Kim, J.A.; Park, J.Y.; Ha, T.K.; Park, D.; Chun, P.; Park, N.H.; Moon, H.R.; Chung, H.Y. A novel synthesized tyrosinase inhibitor: (E)-2-((2,4-dihydroxyphenyl) diazenyl) phenyl 4-methylbenzenesulfonate as an azo-resveratrol analog. *Biosci. Biotechnol. Biochem.* **2013**, *77*, 65–72. [CrossRef] [PubMed]